CHROM. 5895

MOMENTS ANALYSIS IN NON-LINEAR CHROMATOGRAPHY

II. THE SECOND MOMENT

T. S. BUYS AND K. DE CLERK

Chromatographic Research Unit of the South African Council for Scientific and Industrial Research, Department of Physical and Theoretical Chemistry, University of Pretoria, Pretoria (Republic of South Africa)

(Received August 26th, 1971)

SUMMARY

An approximate expression for the peak variance, σ^2, in non-linear chromatography has been derived in terms of a series expansion in the non-linearity parameter, λC_t. Terms that are dependent primarily on flow and effective diffusion, respectively, are found to have opposing effects on σ^2. The predicted trends correlate satisfactorily with the results of a computer simulation of the problem.

INTRODUCTION

The mathematical model which was used to obtain an approximate expression for the first moment in non-linear chromatography[1] has in the present study been extended to a calculation of the effects of non-linearity on the second moment. The results obtained from the model are again checked against a computer simulation of the corresponding non-linear chromatographic system. The basic differential equation is the same as that of the previous work; non-ideal contributions from the stationary phase are consequently not taken into account. This circumstance is not considered to affect the present objective of elucidating the basic facets of the non-linear effects, however, since the contribution from the stationary phase will be essentially analogous to that arising from mobile phase non-ideality. In fact, it is expected to be represented merely by a single additive term in the expression for the second moment.

A SERIES EXPANSION FOR $d\sigma^2/dt$

When the second-moment operator

$$\frac{1}{m_0}\int_{-\infty}^{+\infty}(z-\langle z\rangle)^2\,dz \tag{1}$$

is applied to both sides of the basic differential equation[1]

$$\frac{\partial C}{\partial t} = -\frac{U}{1+\lambda C}\cdot\frac{\partial C}{\partial z} + \frac{D_e}{1+\lambda C}\cdot\frac{\partial^2 C}{\partial z^2} \tag{2}$$

one finds

$$\frac{d\sigma_{nl}^2}{dt} = -I + J - \frac{\sigma_{nl}^2}{m_0}\cdot\frac{dm_0}{dt} \tag{3}$$

where

$$I = \frac{U}{m_0}\int_{-\infty}^{+\infty}(z-\langle z\rangle)^2\cdot\frac{1}{1+\lambda C}\cdot\frac{\partial C}{\partial z}\cdot dz$$

$$J = \frac{D_e}{m_0}\int_{-\infty}^{+\infty}(z-\langle z\rangle)^2\cdot\frac{1}{1+\lambda C}\cdot\frac{\partial^2 C}{\partial z^2}\cdot dz$$

$$\sigma_{nl}^2 = \frac{1}{m_0}\int_{-\infty}^{+\infty}(z-\langle z\rangle)^2 C\,dz$$

$\lambda = 2k_2/(1+k_1)$ is the non-linearity parameter where k_1 and k_2 are defined by the non-linear isotherm

$$n = \varepsilon k_1 C + \varepsilon k_2 C^2$$

The symbols used have, as far as is possible, the same meaning as in ref. 1. A complete list is included at the end of the paper.

Eqn. 3 can be simplified by expanding $1/(1+\lambda C)$ in a binomial series and making use of the fact that C and its first derivative tend to zero as $z \to \pm\infty$. It then follows that

$$\frac{d(\sigma_{nl}^2 m_0)}{dt} = I + J_1 - J_2 + J_3 \tag{4}$$

where

$$I = -2U\sum_{n=1}^{\infty}(-1)^{n+1}\cdot\frac{\lambda^n}{n+1}\cdot\int_{-\infty}^{+\infty}(z-\langle z\rangle)C^{n+1}dz \tag{5}$$

$$J_1 = 2D_e m_0 \tag{6}$$

$$J_2 = 2D_e\sum_{n=1}^{\infty}(-1)^{n+1}\cdot\frac{\lambda^n}{n+1}\cdot\int_{-\infty}^{+\infty}C^{n+1}dz \tag{7}$$

$$J_3 = D_e\sum_{n=1}^{\infty}(-1)^{n+1}n\lambda^n\int_{-\infty}^{+\infty}(z-\langle z\rangle)^2 C^{n-1}\left(\frac{\partial C}{\partial z}\right)^2 dz \tag{8}$$

The form of eqn. 4 is such that (I, J_1, J_2, J_3) are all positive. The linear contribution (*i.e.*, $\lambda = 0$) is seen to be given by $J_1 = 2D_e m_0$ and as $m_0 = m_t$ in this instance, the second moment for linear chromatography is

$$\sigma_l^2 = \sigma_l^2 + 2D_e t \tag{9}$$

The non-linear contributions are therefore seen to arise both from effects associated with the flow velocity, U (the I term), and the effective diffusion, D_e (terms J_2 and J_3).

An approximate analytical expression for the integrals I, J_2, and J_3 can now

be derived by substituting the zeroth-order (*i.e.*, $\lambda = 0$) expression for the concentration distribution. This is the Gaussian distribution

$$C = \frac{m_0}{(2\pi\sigma_1^2)^{\frac{1}{2}}} \cdot \exp - \left[\frac{(z - \langle z \rangle)^2}{2\sigma_1^2}\right] \tag{10}$$

The approximation is further improved by using the actual time-dependent mass per unit cross-section of the mobile phase. m_0 is then given approximately[1] by

$$m_0 = m_1 \left\{1 + \frac{\lambda C_1}{2\sqrt{2}} \left[1 - \frac{1}{\left(1 + \frac{4\pi D_e t}{w_1^2}\right)^{1/2}}\right]\right\} \tag{11}$$

The EG inlet[2] is used to express σ_1^2 as

$$\sigma_1^2 = \frac{w_1^2}{2\pi} + 2D_e t \tag{12}$$

This substitution yields, in general,

$$I = 0 \tag{13}$$

while the second-order expressions for J_2 and J_3 follow as

$$J_2 = \frac{\lambda D_e m_0^2}{(2\sqrt{\pi})\sigma_1} - \frac{\lambda^2 D_e m_0^3}{(3\sqrt{3})\pi\sigma_1^2} \tag{14}$$

$$J_3 = \frac{3\lambda D_e m_0^2}{(8\sqrt{\pi})\sigma_1} - \frac{\lambda^2 D_e m_0^3}{(3\sqrt{3})\pi\sigma_1^2} \tag{15}$$

Integration of eqn. 4 now results in the following second-order expression for σ_{n1}^2:

$$\sigma_{n1}^2 = \sigma_1^2 \cdot \frac{m_1}{m_0} + \frac{\lambda C_1 D_e t m_1}{(\sqrt{2})m_0} - \frac{5\lambda C_1 m_1 w_1^2}{(8\sqrt{2})\pi m_0}\left[\left(1 + \frac{4\pi D_e t}{w_1^2}\right)^{1/2} - 1\right] -$$

$$- \frac{(\lambda C_1)^2 m_1 w_1^2}{16\pi m_0}\left[\left(1 + \frac{4\pi D_e t}{w_1^2}\right)^{1/2} - 1\right] +$$

$$+ \frac{(\lambda C_1)^2 m_1 w_1^2}{32\pi m_0} \cdot \ln\left(1 + \frac{4\pi D_e t}{w_1^2}\right) \tag{16}$$

For the graphical representation and comparison of results, it is convenient to rewrite eqn. 16 in the dimensionless form

$$\frac{\sigma_{n1}^2}{\sigma_1^2} = \frac{\sigma_1^2}{\sigma_1^2} \cdot \frac{m_1}{m_0} + \frac{\lambda C_1 m_1 y}{(2\sqrt{2})m_0} - \frac{5\lambda C_1 m_1}{(4\sqrt{2})m_0}\left[(1 + y)^{1/2} - 1\right] -$$

$$- \frac{(\lambda C_1)^2 m_1}{8m_0}\left[(1 + y)^{1/2} - 1\right] + \frac{(\lambda C_1)^2 m_1}{16m_0} \cdot \ln(1 + y) \tag{17}$$

where

$$y = \frac{4\pi D_e t}{w_i^2}$$

COMPUTER SIMULATION

A computer simulation of eqn. 2 was carried out to test the validity of the theoretical model outlined above. The details of the simulation procedure for an EG inlet[2] is similar to that described previously[1]. Unfortunately, these numerical results differ strikingly from the predictions of the model (eqn. 17) even for small λC_1, as can be seen from Fig. 1 where the non-linear contribution to the reduced second moment has been plotted as a function of the dimensionless time parameter $y = 4\pi D_e t/w_1^2$. A comparison of results from first- and second-order expressions for σ_{n1}^2 revealed that no significant improvement is obtained by the inclusion of higher-order terms which suggests a basic deficiency in the theoretical model.

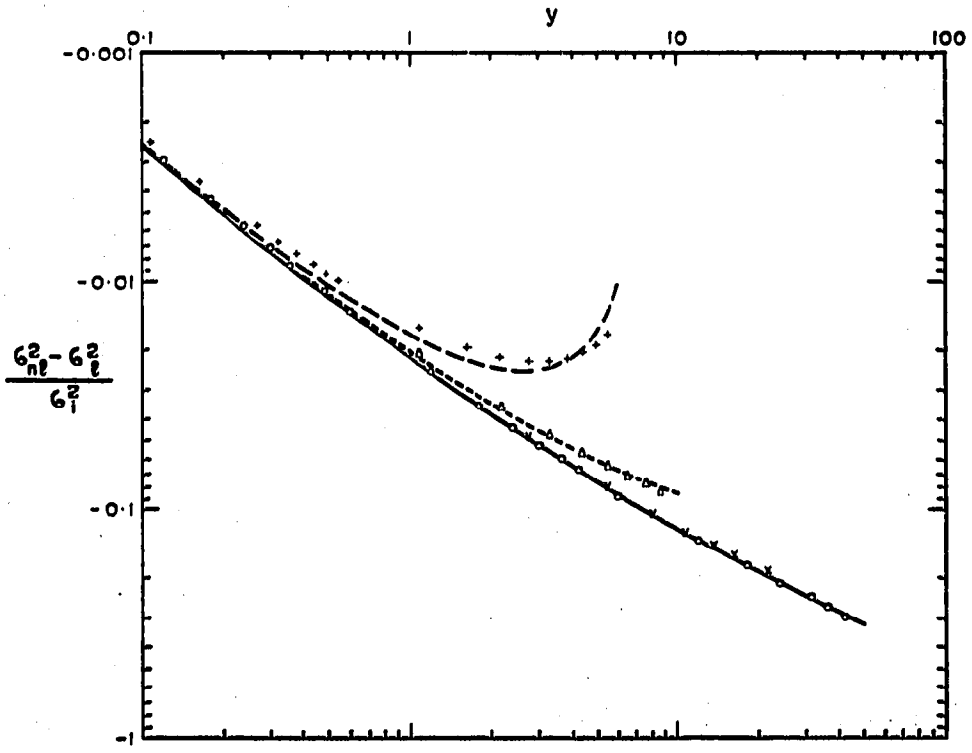

Fig. 1. Comparison of non-linear second moment contributions according to theoretical model and numerical simulation. $\lambda C_1 = 0.1$; $u = 1$ cm/sec; $k_1 = 20$; $w_1 = 4.8$. – – – –, Eqn. 25; $\Omega/8\pi = 0.011$, $D_e = 0.01$. - - - - -, Eqn. 25; $\Omega/8\pi = 0.011$, $D_e = 0.02$. ———, Eqn. 17. +, $D_e = 0.01$; △, $D_e = 0.02$; ×, $D_e = 0.05$; ○, $D_e = 0.110567$.

The most unexpected feature of the simulation results is the occurence of a change of sign in the derivative $d(\sigma_{n1}^2 - \sigma_1^2)/dt$. For example, for $\lambda > 0$, one would expect diffusional spreading to be invariably smaller than in the corresponding linear case owing to the smaller fraction of molecules that are subjected to the effect of D_e. This effect is indeed seen to be present but apparently there exists an additional and opposite effect that becomes more pronounced as D_e is decreased. Inspection of eqn. 4 reveals that I is the only term that can be responsible for such behaviour and a more detailed analysis of this integral is clearly required.

ANALYSIS OF THE FLOW-VELOCITY CONTRIBUTION

As the simple zeroth-order model is suspected to be inadequate in the evaluation of I, an attempt was made to derive a semi-empirical expression for this integral which contains a single empirical parameter. This parameter can then subsequently be adjusted by evaluating the integral numerically. If this parameter is to be constant, however, the complete functional dependence of I on all the relevant parameters is obviously required. An approximate expression for this purpose will now be derived.

This first-order expression for I is given by

$$I = -\lambda U(\int_{-\infty}^{+\infty} ZC^2\,dZ - \langle Z\rangle \int_{-\infty}^{+\infty} C^2\,dZ) \tag{18}$$

where the coordinate transformation $Z = z - Ut$ has been used.

The first of these integrals can be rewritten as

$$\int_{-\infty}^{+\infty} ZC^2\,dZ = \Omega'\langle Z\rangle \int_{-\infty}^{+\infty} C^2\,dZ \tag{19}$$

where Ω' is a dimensionless constant and use has been made of the general mean-value theorem for integrals[3]. Eqn. 18 thus becomes

$$I = -\lambda U\Omega\langle Z\rangle \int_{-\infty}^{+\infty} C^2\,dZ \tag{20}$$

with $\Omega = \Omega' - 1$. For a symmetrical peak $\Omega = 0$, but for an asymmetrical peak $\Omega < 0$. When the integral $\int_{-\infty}^{+\infty} C^2\,dZ$ is approximated by means of the Gaussian distribution (eqn. 10), one finds

$$\int_{-\infty}^{+\infty} C^2\,dZ = \frac{m_0^2}{(2\sqrt{\pi})\sigma_1} \tag{21}$$

while $\langle Z\rangle$ is, to a good approximation[1], given by

$$\langle Z\rangle = -\frac{\lambda C_1 U w_1^2}{(4\sqrt{2})\pi D_e}[(1+y)^{1/2} - 1]\frac{m_1}{m_0} \tag{22}$$

Substitution of eqns. 21 and 22 into eqn. 18 therefore yields

$$I = \frac{\Omega(\lambda C_1)^2 U^2 m_1 w_1^2}{8\pi D_e}\left[1 - \frac{1}{(1+y)^{1/2}}\right] \tag{23}$$

in which the dependence of m_0 on λC_1 has been neglected. For convenience, eqn. 23 is rewritten in the dimensionless form

$$I' = \frac{ID_e}{(\lambda C_1)^2 U^2 m_1 w_1^2} = \frac{\Omega}{8\pi}\left[1 - \frac{1}{(1+y)^{1/2}}\right] \tag{24}$$

In order to test this functional dependence, the I-integral ($n = 1$, eqn. 5) was evaluated numerically for the actual simulated peaks for a variety of λC_1 and D_e values. A graph of I' against $(1+y)^{-1/2}$ should yield a straight line in the small y region [*i.e.*, $(1+y)^{-1/2} \sim 1$]. Inspection of Figs. 2 ($\lambda > 0$) and 3 ($\lambda > 0$) reveals that the correspondence, especially in the latter case, is not perfect; deviations

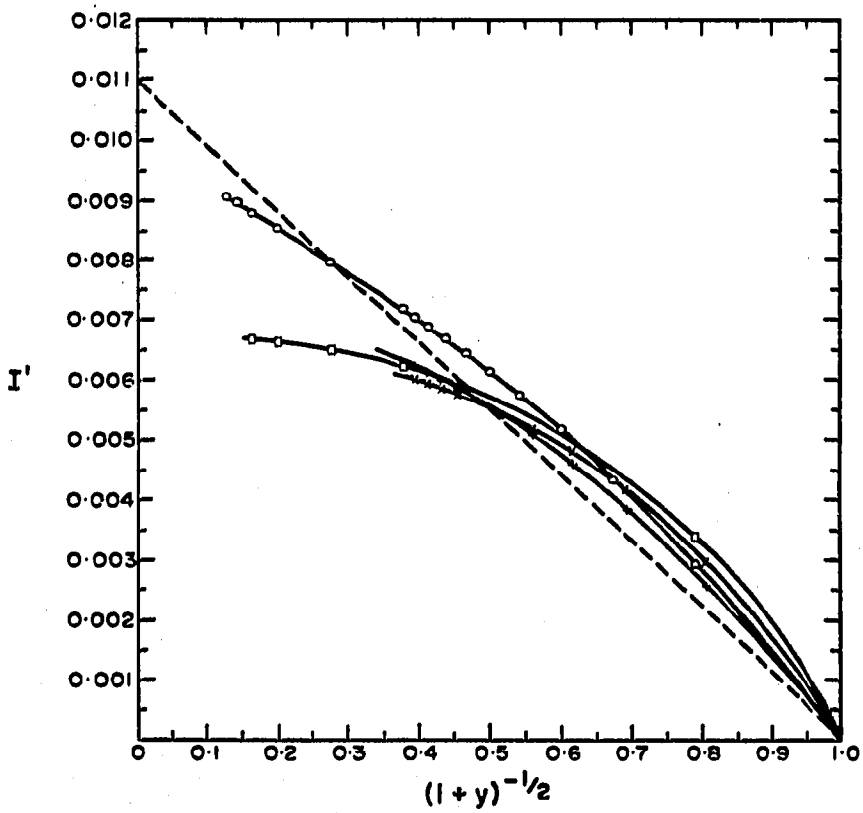

Fig. 2. Flow velocity-dependent contribution to the derivative with respect to time of the second moment. The theoretical prediction (– – – –, eqn. 24) is compared with the results of a numerical evaluation of the I-integral ($n = 1$, eqn. 5). $u = 1$ cm/sec; $k_1 = 20$; $w_1 = 4.8$. – – – –, Eqn. 24; $\Omega/8\pi = 0.011$. ×, $\lambda C_1 = 0.1$, $D_e = 0.01$; +, $\lambda C_1 = 0.5$, $D_e = 0.01$; □, $\lambda C_1 = 0.1$, $D_e = 0.110567$; ○, $\lambda C_1 = 0.5$, $D_e = 0.110567$.

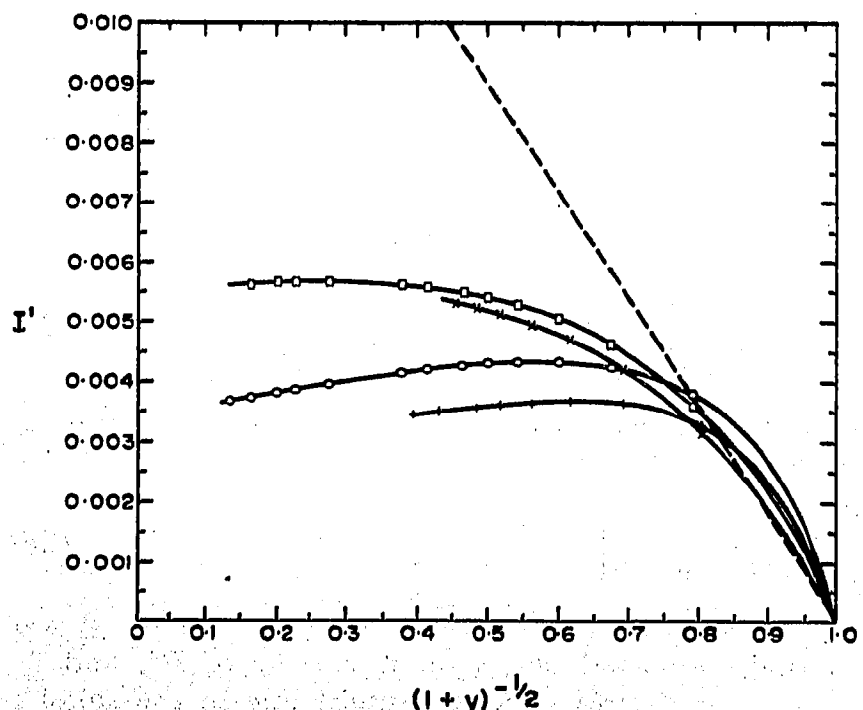

Fig. 3. Flow velocity-dependent contribution to the derivative with respect to time of the second moment. The theoretical prediction (– – – –, eqn. 24) is compared with the results of a numerical evaluation of the I-integral ($n = 1$, eqn. 5). $u = 1$ cm/sec; $k_1 = 20$; $w_1 = 4.8$. – – – –, Eqn. 24; $\Omega/8\pi = 0.018$. ×, $\lambda C_1 = -0.1$, $D_e = 0.01$; +, $\lambda C_1 = -0.5$, $D_e = 0.01$; □, $\lambda C_1 = -0.1$, $D_e = 0.110567$; ○, $\lambda C_1 = -0.5$, $D_e = 0.110567$.

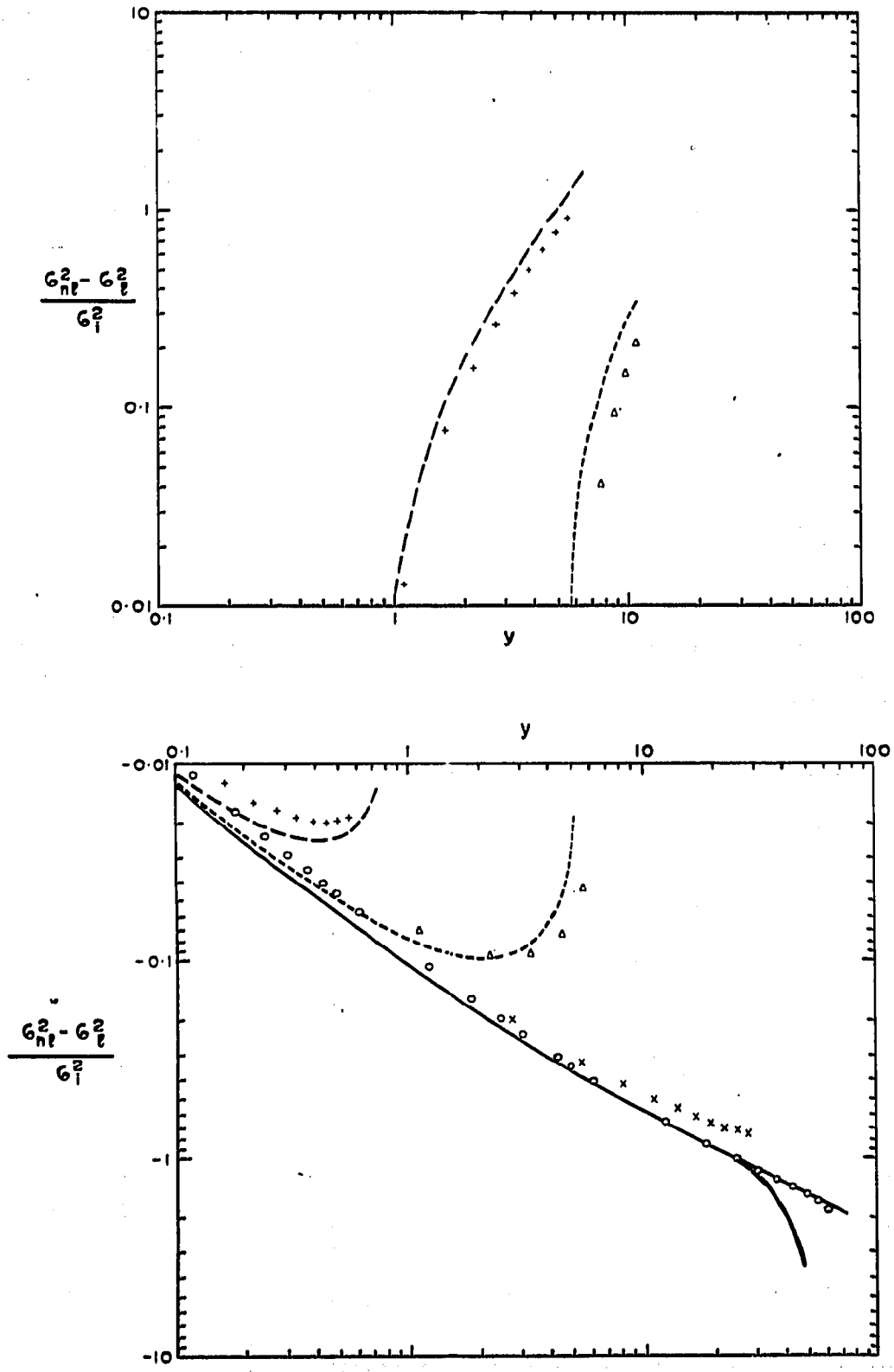

Fig. 4. Comparison of non-linear second-moment contributions according to theoretical model and numerical simulation. $\lambda C_1 = 0.5$; $u = 1$ cm/sec; $k_1 = 20$; $w_1 = 4.8$. – – – –, Eqn. 25; $\Omega/8\pi = 0.011$, $D_e = 0.01$. - - - - -, Eqn. 25; $\Omega/8\pi = 0.011$, $D_e = 0.02$. ———, Eqn. 17. ———, Boundary effect, $C(Z,t) = 0$. +, $D_e = 0.01$; △, $D_e = 0.02$; ×, $D_e = 0.05$; ○, $D_e = 0.110567$.

from the predicted straight line do occur even in the small y region where higher-order effects should become negligible. On the other hand, the test is a stringent one and the numerical significance for σ^2 is of lesser importance than that suggested by Figs. 2 and 3. In essence, the approximately quadratic dependence of this contribution in both λC_1 and U is confirmed. This is in contrast to the diffusion terms J_2 and J_3 which are, to the first order, predicted to be linear in λC_1 and D_e. This latter prediction was successfully verified by numerical integration.

An expression for the reduced second moment including both flow velocity and diffusion terms follows from eqns. 17 and 23 as

$$\frac{\sigma_{n1}^2}{\sigma_1^2} = \frac{\sigma_1^2}{\sigma_1^2}\cdot\frac{m_1}{m_0} + \frac{\lambda C_1 m_1 y}{(2\sqrt{2})m_0} - \frac{5\lambda C_1 m_1}{(4\sqrt{2})m_0}[(1+y)^{1/2} - 1] -$$

$$- \frac{(\lambda C_1)^2 m_1}{8m_0}[(1+y)^{1/2} - 1] + \frac{(\lambda C_1)^2 m_1}{16m_0}\cdot\ln(1+y) +$$

$$+ \frac{\Omega}{8\pi}\cdot\frac{(\lambda C_1)^2 U^2 w_1^2 m_1}{D_e^2 m_0}\left\{\frac{y}{2} - [(1+y)^{1/2} - 1]\right\} \qquad (25)$$

The theoretical values for the non-linear σ^2 contribution which follow from eqn. 25 are compared with the simulation results in Figs. 1 ($\lambda > 0$), 4 ($\lambda > 0$), and 5 ($\lambda < 0$). In the calculation for positive λ, an empirical value of $\Omega/8\pi = 0.011$ was used, while for negative λ, $\Omega/8\pi = 0.018$ was found to be more appropriate.

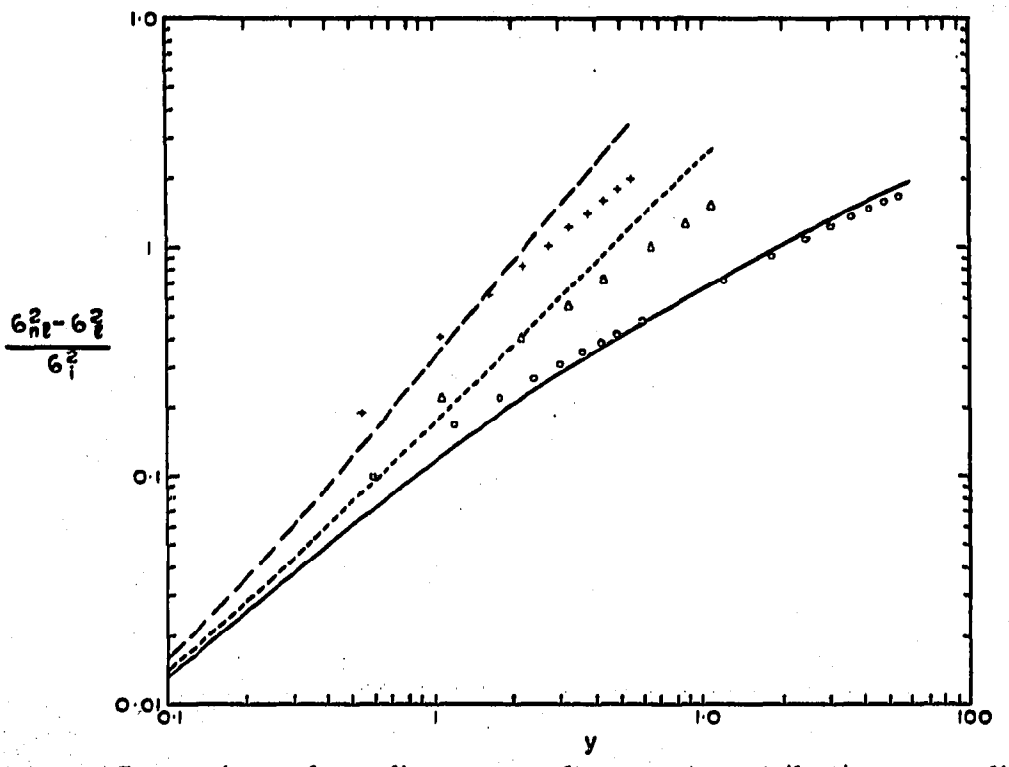

Fig. 5. Comparison of non-linear second-moment contributions according to theoretical model and numerical simulation. $\lambda C_1 = -0.5$; $u = 1$ cm/sec; $k_1 = 20$; $w_1 = 4.8$. – – – –, Eqn. 25; $\Omega/8\pi = 0.018$, $D_e = 0.01$. - - - - -, Eqn. 25; $\Omega/8\pi = 0.018$, $D_e = 0.02$. ———, Eqn. 17. +, $D_e = 0.01$; △, $D_e = 0.02$; ○, $D_e = 0.110567$.

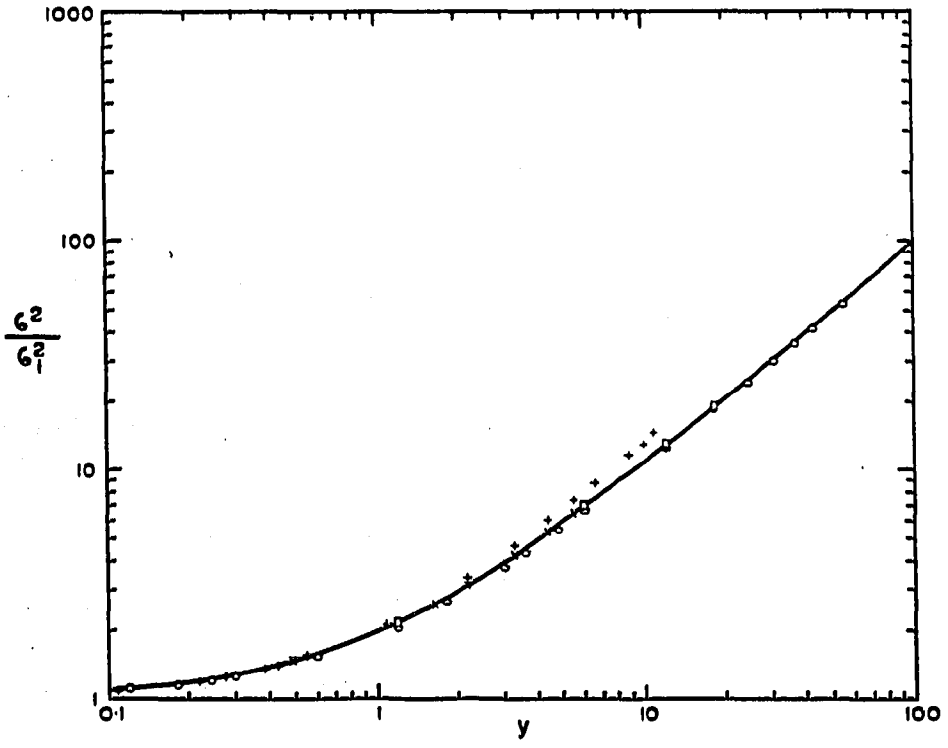

Fig. 6. Illustration of the time-dependence of the linear and non-linear contributions to the total peak variance. $u = 1$ cm/sec; $k_1 = 20$; $w_1 = 4.8$. ———, σ_1^2 (eqn. 11). ×, $\lambda C_1 = 0.1$, $D_e = 0.01$; +, $\lambda C_1 = 0.5$, $D_e = 0.01$; □, $\lambda C_1 = 0.1$, $D_e = 0.110567$; ○, $\lambda C_1 = 0.5$, $D_e = 0.110567$.

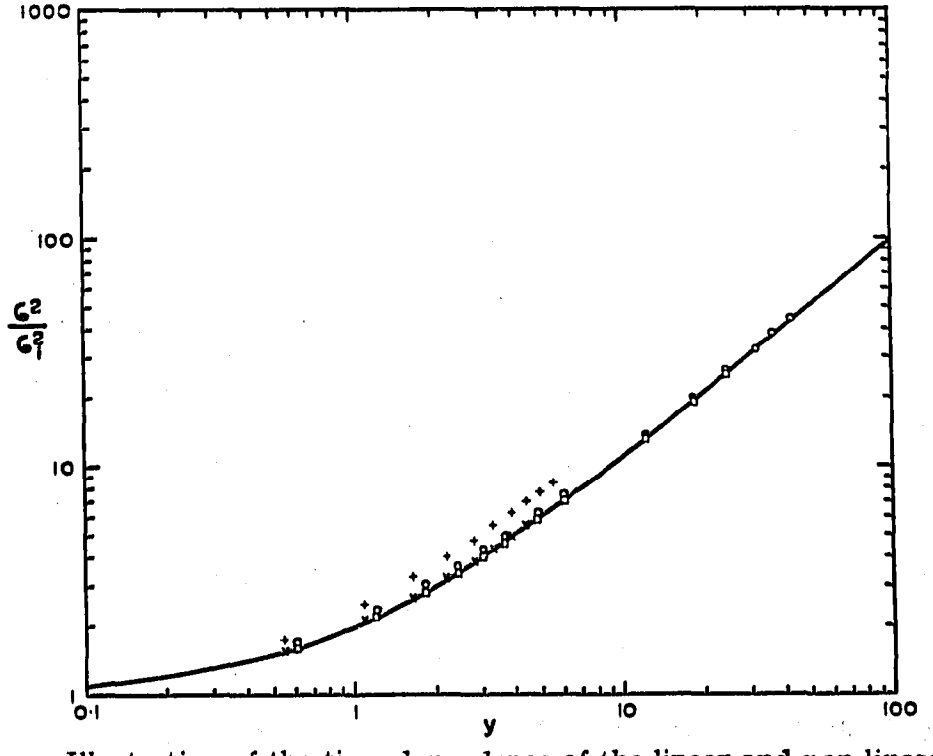

Fig. 7. Illustration of the time-dependence of the linear and non-linear contributions to the total peak variance. $u = 1$ cm/sec; $k_1 = 20$; $w_1 = 4.8$. ———, σ_1^2 (eqn. 11). ×, $\lambda C_1 = -0.1$, $D_e = 0.01$; +, $\lambda C_1 = -0.5$, $D_e = 0.01$; □, $\lambda C_1 = -0.1$, $D_e = 0.110567$; ○, $\lambda C_1 = -0.5$, $D_e = 0.110567$.

DISCUSSION

The opposing non-linear contributions of flow and diffusion to peak variance are summarized in Figs. 1, 4, and 5. The success of the model calculations in predicting these deviations can now be gauged by comparing them with the simulation results.

The relatively large deviations of model results from simulation results observed for negative λ in Fig. 5 are most probably due to the more complicated actual functional form of the flow-velocity term in this case (see Fig. 3). It is clear, however, that the attendant phenomena are at least qualitatively well understood. In assessing the quantitative merit of the theoretical predictions, one should keep in mind that the results are presented in such a way as to accentuate any discrepancies. On a scale comparable with the linear peak variance contributions, the non-linear effects are ordinarily quite small, as can be seen from typical cases for positive and negative λ depicted in Figs. 6 and 7. This statement becomes invalid when the parameter $\lambda C_1 U w_1/D_e$ (eqn. 25, last term) becomes large enough for the non-linear contribution to become comparable to the linear σ_{n1}^2 contribution. This will be the case for columns with a small D_e value (*i.e.*, a small linear plate height, H_1). An approximate criterion for assessing the relative contributions is found by setting the two contributions equal to each other. H_1 defined by

$$H_1 = \sigma_1^2/Ut \approx 2D_e/U$$

is for this point then found to be given[4] by

$$H_1 = \left(\sqrt{2\,\frac{\Omega}{8\pi}}\right)\lambda C_i w_i$$

where the approximation of large y values has been used.

An idea of the accuracy required to calculate these non-linear effects is provided by a consideration of the amount of cut-off which is allowed. In a typical instance, the boundary condition $C(Z,t) = 0$ for $|Z| > 40$ cm was found to cut off all values of $C < 0.168\,\%$ of C_{max}. This yielded the sharply curving bold line in Fig. 4a. Increase of the Z range to $|Z| > 60$ cm changed the boundary condition to $C < 0.00045\,\%$ of C_{max}. and resulted in the solid line, which shows that the excessive curvature of the bold line was due, not to a physically significant phenomenon, but merely to an invalid numerical approximation. Unfortunately, accuracy is limited by the computing time available. For instance, in the example cited above, the increased accuracy was only obtained at the expense of a 50 % increase in computing time and as 1 sec of computing time in the present analysis corresponds roughly to 1 sec of elution time, further refinement of the simulation results become unrealistic.

SYMBOLS

C = mass of solute per unit mobile phase volume
C_1 = value of C at $t = 0$ at the inlet
D_e = $D_p/(1 + k_1)$
D_p = effective diffusion coefficient

I = convenient parameter, eqn. 3
I' = convenient parameter, eqn. 24
J = convenient parameter, eqn. 3
J_1 = convenient parameter, eqn. 6
J_2 = convenient parameter, eqn. 7
J_3 = convenient parameter, eqn. 8
k_1 = parameter in adsorption isotherm
k_2 = parameter in adsorption isotherm
m_0 = zeroth moment
m_1 = mass of solute per unit cross-section of the mobile phase at inlet at time $t = 0$
n = mass of solute adsorbed per unit column volume
t = time
U = $u/(1 + k_1)$
u = carrier flow velocity
w_1 = width of plug inlet sample profile
y = $4\pi D_e t/w_1^2$; dimensionless time parameter
z = axial coordinate
$\langle z \rangle$ = first moment of concentration–distance distribution
Z = $z - Ut$; relative axial coordinate
$\langle Z \rangle$ = $\langle z \rangle - Ut$

Greek symbols

ε = void fraction
λ = non-linearity parameter (eqn. 2)
σ^2 = total variance
σ_1^2 = inlet variance
σ_l^2 = total variance in linear chromatography
σ_{nl}^2 = total variance in non-linear chromatography
Ω = convenient parameter, eqn. 20
Ω' = convenient parameter, eqn. 19

REFERENCES

1 K. De Clerk and T. S. Buys, *J. Chromatogr.*, 63 (1971) 193.
2 K. De Clerk, T. S. Buys and V. Pretorius, *Sep. Sci.*, 6 (1971) 733.
3 G. A. Korn and T. M. Korn, *Mathematical Handbook for Scientists and Engineers*, McGraw-Hill, New York, 1961.
4 T. S. Buys and K. De Clerk, *J. Chromatogr.*, in press.